Statistical analysis of a set of Parisian Concert Halls and Theatres

J.-D. Polack, F. Leão Figueiredo and S. Liu

LAM/IJLRA - Université Pierre et Marie, 11 rue de Lourmel, 75015 Paris, France
jean-dominique.polack@upmc.fr

During the year of 2009, the room acoustics group of the LAM (Équipe Lutheries, Acoustique, Musique at Institut Jean Le Rond d'Alembert - Université Pierre et Marie Curie, Paris) performed a series of acoustical measurements in music halls in Paris. The halls were chosen in regarding their importance to the historic, architectural or acoustic domains. The measured ensemble of fourteen rooms includes quite different architectural designs. The measurements were made both in empty and in occupied rooms, and a comprehensive series of statistical analysis was carried out to fully characterize the database thus obtained. The presentation briefly describes the protocol, then moves on to the statistical analysis. The results obtained draw new insight into the structure of room acoustical measurements, and will be compared with results from the literature.

1 Introduction

During the year 2009, the room acoustics group at LAM (Équipe Lutheries-Acoustique-Musique, Institut Jean Le Rond d'Alembert, Université Pierre et Marie Curie, Paris) performed a series of acoustical measurements in concert halls and theatres in Paris. The halls and theatres were selected for their historical, architectural, or acoustic interest.

A systematic protocol for checking room-acoustical measurement procedures was set up. The influence on acoustical indices of varying source directivity, acoustics configuration, and pre-equalized excitation signals, has been published previously [4]. Therefore, in the present paper, we focus on the statistical analysis of the measured acoustical indices, in order to evaluate the relevance of acoustical indices described in ISO Standard 3382 [5].

2 Measuring equipment

2.1 Source

The measuring equipment consists of a dodecahedral sound source (*Outline GSR*), and a subwoofer (*Tannoy Power VS10*) connected to the source, both supplied with their amplifiers.

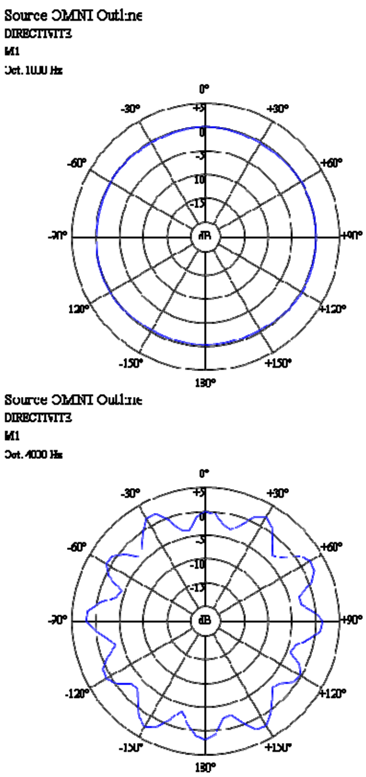

Figure 1: Polar responses of the source at 1kHz and 4kHz.

At its frequency of operation, the subwoofer radiation is omnidirectional, and so is the dodecahedron up to the 1kHz octave, as depicted in Figure 1. However, at higher frequencies, the directivity departs from omnidirectionality, but variations remain within 5dB in the highest octave band considered by ISO Standard 3382 (Figure 1).

2.2 Microphone

All measurements were carried out an Ambisonics SoundField ST 250 microphone, connected to a multichannel soundcard driven by a laptop.

The Soundfield microphone contains four sub-cardioid capsules mounted in a tetrahedral arrangement. By combining the output of the four capsules, a pressure microphone and three gradient microphones, at right angles from each other, can be reconstructed. This four-channel signal is known as the Ambisonics B-Format.

Figure 2 presents the pressure responses of the pressure microphone (upper trace) and the gradient microphones (lower trace) reconstructed from the SoundField ST250. The omnidirectional response is constant within 1dB from 60Hz to 4kHz, and the figure-of-eight response with ±1dB within the same range, extending in fact up to 2kHz.

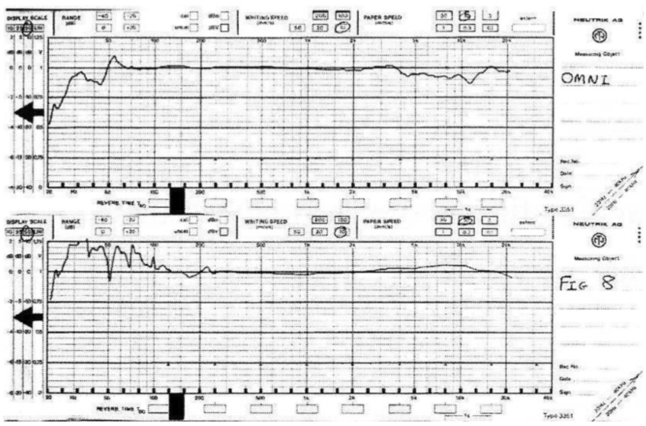

Figure 2: Responses of ST250 microphone.

2.3 Signal

An exponential sweep-sine signal was used as original signal, because it allows *a posteriori* elimination of harmonic distortions from the sound source, as well as efficient signal-to-noise ratio [3,7]. It was recorded and processed with the Aurora plug-ins, developed by Angelo Farina from Parma University.

The sweep sine signal is generated 20 Hz up to 20 kHz in 30 seconds. A relatively long duration was selected because the signal-to-noise ratio is proportional to the sweep time.

Figure 3 presents the spectrum of the sweep signal radiated in the large anechoic chamber at LNE (upper trace) together with the spectrum of the compensated sweep signal (intermediate trace). Evident in Figure 3 is the fact that compensation allows rectifying the signal over a large band, from 60Hz to 5.5kHz, that is, for the band covered by ISO Standard 3382 [5]. However, post processing makes it possible to further extend the bandwidth from 40Hz to 18kHz, at the cost of a light reduction in the level (lower trace in Figure 3). This extra bandwidth is necessary in the case of auralisation only, but not for measuring indices.

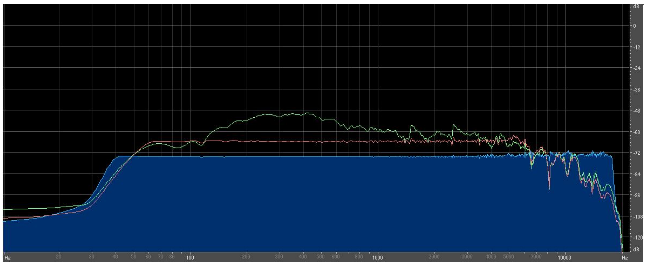

Figure 3: Original spectrum of the signal and the two steps of compensation.

For all measurements, the compensated signal was radiated in the halls, since we are only interested in the indices.

3 Measurement protocol

3.1 The 14halls

The halls were selected for their historical, as well as architectural and acoustic interests.

Table 1: The 14 halls.

	Volume (m3)	Seats	Abbr.
Théâtre des Abbesses	4500	396	ABE
Théâtre de l'Athénée	3366		ATH
Opéra Bastille	26000		BAS
Chapelle Royale de Versailles	14400		CHP
Théâtre du Châtelet		2300	CHT
Cité de la Musique	13400	1200	CIT
Salle Cortot	2580	400	COR
Opéra Garnier			GAR
Maison de la Culture du Japon	6300	400	JAP
Auditorium du Louvre	4500		LOU
Théâtre de la Porte St. Martin		1000	MAR
Auditorium du Musée d'Orsay	1700	347	ORS
Salle Pleyel	17800		PLE
Maison de Radio France	10000		RAD
Théâtre du Ranelagh	1920		RAN
Théâtre de la Ville	5120	1012	VIL

As our goal was not to evaluate acoustical excellence, but rather the acoustical criteria, we were looking for a representative set of halls with broad ranges of such characteristics as: volume, form, wall materials, number of seats, and artistic usage.

Table 1 lists the 14 halls selected for the campaign, together with their volumes and numbers of seats. It also indicates the abbreviations used to refer to them.

3.2 Positions

In each hall, ten microphone positions were selected (except for the smaller rooms, as indicated in ISO standard 3382), trying to preserve a standard distribution of positions while respecting the physical possibilities of the rooms. Microphone positions were therefore selected according to the follow scheme:

- Positions 'a', 'b' and 'c' on the central longitudinal axis ('a' nearest and 'c' furthest from stage).
- Positions 'd' and 'e' on lateral longitudinal axis ('d' nearer and 'c' further from stage).
- Positions 'f' and 'h' on central longitudinal axis, first and second balcony respectively.
- Positions 'g' and 'j' on lateral first and second balcony, respectively.

Other positions were used occasionally, depending on architectural specificities of the rooms. As for the source, it was positioned on the centre of the stage. For microphone positions on longitudinal axes, left and right positions of the source (LR) were also used.

4 Indices and their distribution

4.1 Indices

For each measurement position, a set of indices was computed following the list recommended by ISO Standard 3382 [5]. They are listed in Table 2.

Table 2: The indices.

Indices	Formules
T30 (s)	2.[t (-35dB) - t (-5dB)], $E(t)=\int_t^\infty p^2(\tau)d\tau$
EDT (s)	6.[t (-10dB) - t (0dB)], $E(t)=\int_t^\infty p^2(\tau)d\tau$
Ts (ms)	$\left[\int_0^\infty t.p^2(t)dt \Big/ \int_0^\infty p^2(t)dt\right]$
G (dB)	$10\log\left[\int_0^\infty p^2(t)dt \Big/ \int_0^\infty p^2_{10m}(t)dt\right]$
C80 (dB)	$10\log\left[\int_0^{80ms} p^2(t)dt \Big/ \int_{80ms}^\infty p^2(t)dt\right]$
LF	$\left[\int_{5ms}^{80ms} p^2_{lat}(t)dt \Big/ \int_0^{80ms} p^2_{omni}(t)dt\right]$

Additional indices were also computed, such as the bass ratio BR (ratio of the mean reverberation time at 125Hz and 500Hz, over the mean reverberation time at 500Hz and 1kHz), and the treble ratio TR(ratio of the mean reverberation time at 2kHz and 4kHz, over the mean reverberation time at 500Hz and 1kHz). Both were introduced by Beranek [2].

4.2 Distributions

Following the recommendation of Bech and Zakharov [1], we first checked the distributions of all indices, for each octave bands. Figures 4 and 5 presents two examples, for the mean values over all octave bands of two indices: C80, and T30.

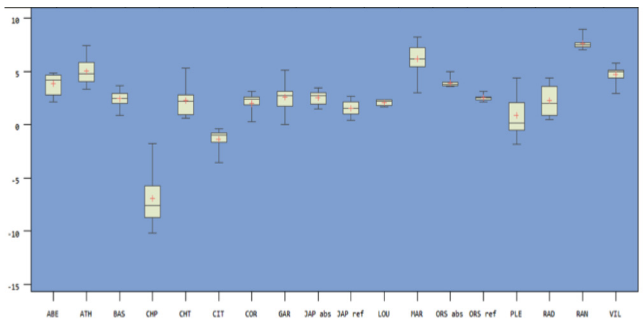

Figure 4: Box plots for mean C80.

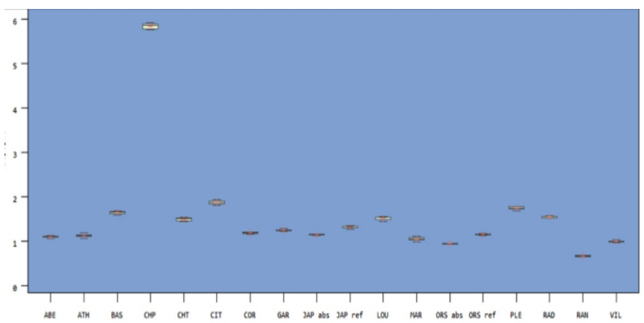

Figure 5: Box plots for mean T30.

Most of the Box plots are similar to Figure 4: they present large variations within single halls, and strong overlaps across halls. On the other hand, reverberation time T30 behaves differently, since its value is fairly constant within single halls (Figure 5). However, reverberation time can be similar in different halls, even if their sizes and types are very different as is the case for Opéra Garnier and Salle Cortot. As a consequence, one index cannot characterize halls on its own, and one has to consider the set of all indices to carry out classification.

5 Multivariate analysis

When considering all indices measured and all octave bands, a total of 55 values are obtained for characterizing each measurement position in each hall. Such a large, high-dimensional data set presents a challenge for visualization and analysis.

Since visualization is impossible beyond a few dimensions, the data set has to be reduced. Even when aggregating all octave results in one mean value for each index, this only reduces the data set to 13 dimensions, far too much for visualization. As a result, multivariate analysis methods must be called in.

All multivariate methods have in common that they project the data on an orthonormal set iteratively obtained by selecting at each step the direction of maximum extension of the data set, then reducing the dimension by considering the orthogonal space.

5.1 Cluster analysis

Cluster analysis is a method of partition which aims at dividing a whole of data into various homogeneous groups so that the data of each subset share common characteristics. Such characteristics generally correspond to criteria of proximity (similarity) that are defined by introducing distance measurements and classes between objects [9]. To obtain good partitioning, one must simultaneously:

- minimize intra-class differences to obtain clusters as homogeneous as possible,
- maximize inter-class differences.

k-means is an iterative method of classification. One specifies the number k of groups to be obtained, calculations are repeated several times and the optimal solution is selected. The first iteration starts with selecting, at random or not, k objects that feature the centres of the k classes. The distance between all the objects and the k centres are then calculated, and objects are aggregated to closest centre. The next step consists in redefining the centres as each class as its barycentre. Several iterations are necessary to reach convergence.

Figure 6 presents the clusters obtained for an analysis in 6 classes, projected on the plane defined by the two first axes of canonical discrimination, that is, the linear combinations of the 10 standardized variables which maximize the ratio of the between-group variation to the within-group variation of the 6 classes. In fact, we started with 7 classes, but found out that class 6, corresponding only to Chapelle Royale, was very far from the others because of high reverberation time (see Figure 5). This is why class 6 does not appear in Figure 6. Two groups of two classes overlap in Figure 6: classes 2 and 7, and classes 3 and 5. They are signalled by circles. Therefore, we chose to combine these classes, obtaining 5 classes corresponding to: medium-size theatres; opera houses; medium-size auditoria; concert halls; Chapelle Royale.

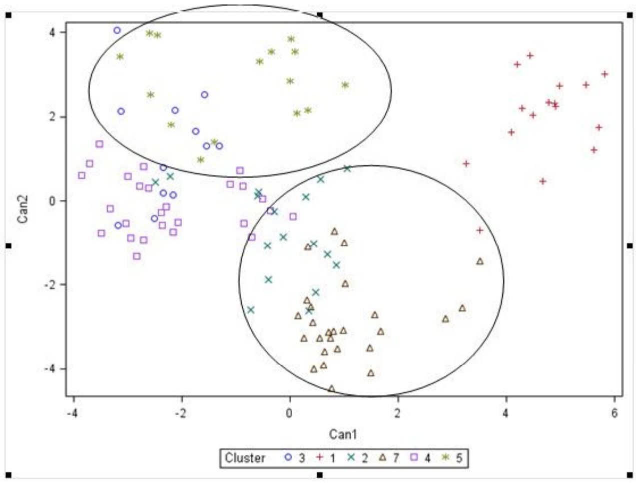

Figure 6: First two axes of canonical discriminations for clustering in 7 classes.

The interesting result is that cluster analysis of the measurement data leads to a classification that corresponds to the traditional typology of halls. This proves the relevance of our corpus of halls, as well as the relevance of the selected indices for characterizing concert halls. Furthermore, discrimination of the clusters is maximal along the indices T30, Ts and C80.

5.2 Correlation analysis

In order to examine whether there exists a connection between two sets of data *x* and *y*, one represents each observation *i* as a point of coordinates (x_i , y_i) in a Cartesian coordinate system. The shape of the cloud thus obtained reveals the existence of a correlation not. In the first two plots of Figure 7, data are concentrate along one of the diagonals, corresponding to a linear relationship between the two indices; the goodness of fit is measured by the dispersion around the line, or by the correlation coefficient R-*square* which reaches values close to 1 when the dispersion is small. On the other hand, the dispersion is large, and R is small, when the data spreads over the plot, as in the last plot in Figure 7.

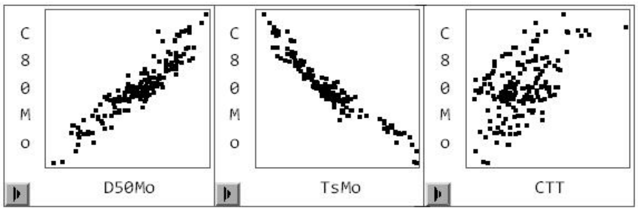

Figure 7: Examples of correlations between indices.

Table 3 lists the principle correlations between indices observed in our database, and compares them with results from the literature [6,8]. It is obvious that results are similar, except for the correlations with T30 in Pelorson's study [8]. The difference may lie in the differences between measurement protocols, as measurement positions were chosen at random by Pelorson, but not by Julien who used a systematic grid similar but more comprehensive than ours.

Table 3: Principle correlations.

R-*square*	this study	Pelorson	Jullien
T30 x EDT	0.91	0.65	0.93
T30 x C80	-0.78	-0.53	-0.74
T30 x Ts	0.85	0.55	0.90
EDT x C80	-0.82	-0.91	-0.88
EDT x Ts	0.84	0.94	0.98
C80 x Ts	-0.95	-0.95	-0.91

The main result from correlation analysis is that it confirms the close relationship between indices T30, Ts and C80 revealed by the cluster analysis.

5.3 Principal Component Analysis

The idea behind Principal Components Analyses (PCA) is to account for the variance observed in a cloud of data by limiting the number of components, defined as simple mathematical transformations of the initial variables.

Principal Components Analyses (PCA) were carried out for a variety of sets of indices, including octave values. Figure 8 presents the mean octave values of the indices in the plane built by the two principal components. Each of the 13 indices is represented in this plot by a point, and the direction and the distance from origin of the point indicates how each index contributes to the two principal components in the plot.

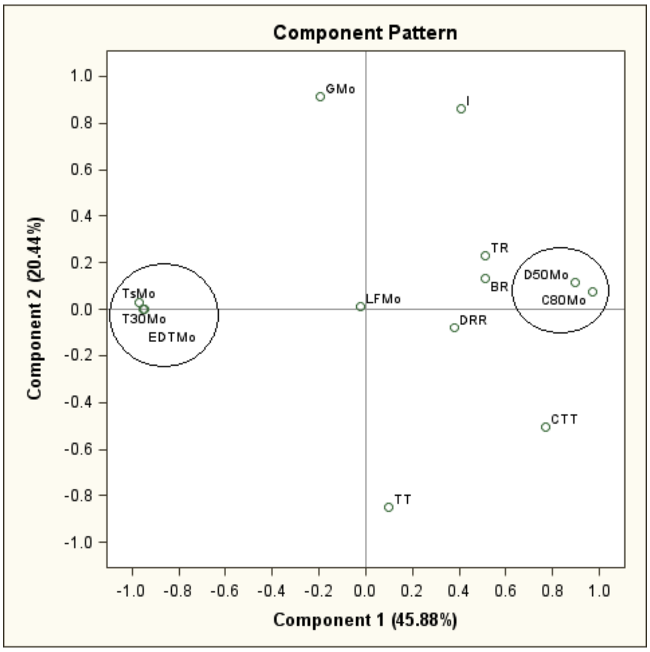

Figure 8: PCA for mean octave values of the indices

It can be seen in Figure 8 that the group formed by T30, EDT Ts and C80 strongly contributes to the first component. As this first component accounts for 46% of the variance of the data, these indices dominate the spreading of the data. This result is in agreement with the earlier finding that the same indices constitute the principal discrimination variables for clustering analysis (see Section 4.1). Index G contributes to the second component, which accounts for 20.5% of the variance. The complete PCA reveals that the third component accounts for 12.5% and the fourth component 9% of the variance. Thus four components are sufficient to explain as much as 88% of the variance of our database.

Figure 8 also enables us to visualize the correlations between the indices: indices closer to each other, or symmetric with respect to the origin, are better correlated. Thus, distant but symmetrical indices like Ts and C80 are strongly (and negatively) correlated. It is another way of observing the same correlations as observed in Sections 4.1 and 4.2.

The first two principal components of the PCA for the present complete set of halls are very similar to the ones that Pelorson derived for the PCA of his complete set of halls [8]. Therefore, we believe that the present results can be extrapolated to any large set of halls. However, PCA for a particular hall can give very different results, as shown by the same Pelorson.

6 Conclusion

The statistical analysis presented in this paper, and its comparison with similar analyses, prove that the present database is representative of the variety of concert halls and theatres known in the literature: the principles components are the same. This finding validates our principles for selecting the halls, as well as the measurement protocol designed for the present study. Further, the present study validates the indices recommended by ISO Standard 3382, since these indices can discriminate the corpus of halls.

Acknowledgments

The authors thank the management of all the halls for granting permission to carry out acoustical measurements. They also thank Jacques Poitevineau for fruitful advices on statistical analysis. This work is part of a doctorate thesis supported by the "Coordenação de Aperfeiçoamento de Pessoal de Nível Superior (CAPES)" of the Ministry of Education of Brazil.

References

[1] S. Bech, N. Zakharov, *Perceptual, audio, evaluation, Theory, method and application*, Wiley, Chichester, (2006)

[2] L.L. Beranek, *Concert and Opera Halls. How they sound*, Acoustical Society of America, New York (1996)

[3] A. Farina, P. Fausti, R. Pompoli, "Measurements in opera houses: comparison between different techniques and equipment." *Proc. of ICA98 - International Conference on Acoustics*, Seattle (1998)

[4] F. Leao Figueiredo, J.D. Polack, "Variations on acoustical measurement procedures and their influence on acoustical parameters", *ISRA 2010*, Melbourne (2010)

[5] ISO 3382 Acoustics, *Measurement of the reverberation time of rooms with reference to other acoustical parameters* (1997)

[6] J.P. Jullien, "Structured model for the representation and the control of room acoustical quality, *Int. Congr. Acoustics*, Trondheim, Norway (1995)

[7] S. Müller and P. Massarani, "Transfer Function Measurements with Sweeps", *Journal of the Audio Engineering Society* **49**(6), 443 (2001)

[8] X. Pelorson, J.P. Vian, J.D. Polack, "On the variability of room acoustical parameters: reproductibility and statistical validity", *Applied Acoustics* 37, 175-198 (1992)

[9] G. Saporta, *Probabilités, analyse des données et statistique*, Ed.Technip (1990)